

Infrared reflectance spectrum of BN calculated from first principles

Yongqing Cai*, Litong Zhang, Qingfeng Zeng, Laifei Cheng, Yongdong Xu

National Key Laboratory of Thermostructure Composite Materials, Northwestern Polytechnical University, Xi'an, Shannxi 710072, PR China

Received 17 October 2006; accepted 30 October 2006 by A.H. MacDonald

Available online 15 November 2006

Abstract

Using the linear response theory, vibrational and dielectric properties are calculated for *c*-BN, *w*-BN and *h*-BN. Calculations of the zone-center optical-mode frequencies (including LO–TO splittings) are reported. All optic modes are identified and excellent agreement is found between the theory and experimental results. The static dielectric tensor is decomposed into contributions arising from individual infrared-active phonon modes. It is found that all the structures have a smaller lattice dielectric constants than those of the electronic contributions. Finally, the infrared reflectance spectrums are presented. Our theoretical results indicate that *w*-BN shows a similar reflectivity spectrum as *c*-BN. It is difficult to tell apart the wurtzite structure from the zinc blende phase by IR spectroscopy.

© 2006 Elsevier Ltd. All rights reserved.

PACS: 78.30.-j; 77.84.Bw; 63.20.-e

Keywords: A. BN; C. Infrared reflectance spectrum; E. First principles

1. Introduction

Boron nitride is one of the most important materials among the III–V compounds due to its chemical, mechanical and electronic properties. High bulk modulus, high thermal conductivity and low dielectrics have seen *c*-BN being used as protective coating films and in modern microelectronic devices at high temperatures. Being a very good electrical insulator with good thermal conductivity and stability, *h*-BN has been widely used in nuclear energy and vacuum technology [1].

Boron nitride is known to have three main polytypes: the cubic phase (*c*-BN) with zinc blende structure is the thermodynamically stable phase under ambient conditions, the wurtzite structure (*w*-BN) is metastable above a pressure of 10 GPa [2], which resembles hexagonal diamonds, the hexagonal structure of BN (*h*-BN) is similar to the structure of graphite. Infrared reflectivity (IR) measurement may be considered a powerful tool for the quantitative analysis of these structures. Geick et al. [3] investigated the reflection and transmission spectrum in the spectral range from 400 to 50 000 cm^{−1}, and two *h*-BN structures with different stacking

sequences of the hexagonal BN layers were discussed. Gielisse et al. [4] recorded the infrared reflection spectrum of cubic boron nitride between 400 and 1800 cm^{−1}. However, as far as we know, there have been no such experiments on the wurtzite modification.

First-principles calculations based on the density-functional theory complement experiments and are useful for predicting the ground-state properties of materials using no experimental values. Extensive theoretical studies have been performed on the electronic and structural properties of BN [5,6]. For its dielectric properties, the static dielectric constants of the three polytypes were calculated with the ultrasoft pseudopotential method and the linear response approach based on the density-functional perturbation theory [7]. However, to our best knowledge, there has been no theoretical study on the infrared reflectance spectrum for the three modifications of BN (*c*-BN, *w*-BN and *h*-BN).

In this work, we present the results of first-principles calculations on the vibrational and dielectric properties for *c*-BN, *w*-BN and *h*-BN through the linear response approach. The calculated infrared reflectance spectrums are reported. In Section 2, we briefly describe the technical aspects of our calculations. Section 3 presents the results, including the structural relaxations, the phonon normal modes, the dielectric

* Corresponding author.

E-mail address: npucai@163.com (Y. Cai).

tensors, and the theoretical IR reflectance spectrums. Section 4 concludes the paper.

2. Details of first-principles calculations

The calculations are carried using the CASTEP [8,9] code with norm-conserving pseudopotentials [10]. We employ the Ceperley–Alder [11] local density functional potential as parameterized by Vosko et al. [12]. The 2s and 2p semicore shells are included in the valences for both N and B. The kinetic energy cutoff for the plane waves is 550 eV. Integrals over the Brillouin Zone are approximated by sums on $(10 \times 10 \times 10)$, $(9 \times 9 \times 6)$ and $(9 \times 9 \times 4)$ Monkhorst–Pack k-point meshes [13] for *c*-BN, *w*-BN and *h*-BN, respectively.

The first-principles investigation of vibrational and dielectric properties are performed within the linear response theory [14]. Γ -phonon frequencies and dielectric tensors are computed as second-order derivatives of the total energy with respect to atomic displacements or an external electric field. Technical details can be found in [15,16]. To obtain the LO/TO splitting characteristic for the three polytypes, we introduced to the dynamical matrix the non-analytical term proposed by Pick [17].

3. Results and discussion

The calculation starts with an optimization of the lattice constants and the internal coordinates to obtain the minimal energy structural model. Both the lattice constants and the internal coordinates are relaxed by calculating the ab initio forces on the ions until the absolute values of the forces converge to less than 0.01 eV/Å. For the *c*-BN and *h*-BN case, the minimum energy configurations are determined by relaxing the lattice constants only, whereas in the *w*-BN case, the energy is related to both the lattice constants and an internal parameter *u*, which characterizes the relative length of the B–N bonds parallel to the *c* axis.

The optimized structural parameters are listed in Table 1. It can readily be seen that there is excellent agreement between our results and results from the previous experiment, except for the lattice constant of *h*-BN. For the latter, our calculated value is 6.378 Å whereas the corresponding reported value in Ref. [20] was 6.660 Å. The relatively large discrepancy of the lattice constant *c* is due to the Van der Waals interaction between the sheets, which is not properly described either in the LDA or the GGA [21]. It should be noted that an overall underestimation of the lattice constants in comparison with experimental results is typical of LDA calculations.

Since primitive unit cells of BN structures have 2 atoms for *c*-BN, and 4 atoms for both *w*-BN and *h*-BN, the corresponding numbers of vibrational modes are 6 and 12, respectively. Our group theoretical analyses indicate that the optical modes at the Γ point can be decomposed as

$$\Gamma_{\text{vib}} (\text{cubic}) = T_2(R, \text{IR})$$

$$\Gamma_{\text{vib}} (\text{wurtzite}) = A_1(R, \text{IR}) + E_1(R, \text{IR}) \\ + 2E_2(R) + 2B_1 (\text{silent})$$

$$\Gamma_{\text{vib}} (\text{hexagonal}) = A_{2u}(\text{IR}) + E_{1u}(\text{IR}) \\ + 2E_{2g}(R) + 2B_{1g} (\text{silent}).$$

Table 1

Calculated and experimental structural parameters for the three polytypes of BN: lattice constant *a*, *c* (Å), internal parameter *u*, and inequivalent atomic positions

<i>a</i>	<i>c</i>	<i>u</i>	Cation (B)	Anion (N)	
<i>c</i> -BN					
3.592			0, 0, 0	1/4, 1/4, 1/4	Present
3.615					Expt. ^a
<i>w</i> -BN					
2.531	4.189	0.3746	1/3, 2/3, 0	1/3, 2/3, <i>u</i>	Present
2.553	4.228				Expt. ^b
<i>h</i> -BN					
2.491	6.378		1/3, 2/3, 1/4	2/3, 1/3, 1/4	Present
2.504	6.660				Expt. ^c

^a Ref. [18].

^b Ref. [19].

^c Ref. [20].

For *c*-BN, there is a bond stretching T_2 mode at the center of the Brillouin zone, which is active in both Raman and IR spectroscopy. In the case of the wurtzite and hexagonal structures, the IR modes group into modes with displacements either in the *x*, *y* plane or along the *z* direction. The E_1 and E_{1u} modes have displacement patterns in the *x*, *y* plane, whereas the A_1 and A_{2u} modes have displacements along *z*. Due to inversion symmetry, the IR and Raman modes are mutually exclusive for *h*-BN.

Values of the calculated optical phonon frequencies are listed in Table 2. They are compared with experimental data from first-order Raman or IR spectroscopy [2,22,23] as well as with results from a previous first principles calculation using ultrasoft pseudopotentials method and the linear response approach [7]. Our calculations present a root mean square absolute deviation of 21 cm^{−1}, and an rms relative deviation of 6.5% with respect to the measurements. The “missing” E_{2g} mode in Ref. [2] is identified, which was previously believed to be in the low frequency region of the spectrum due to the small Van der Waals forces between adjacent flat B₃N₃ hexagons layers. No experimental data are available for *w*-BN; however, the agreement of our calculations with other theoretical investigations for the modes at the Γ point is reasonable [7].

Crystal symmetry leads the dielectric tensors to be composed of some independent components. In the cubic phase, ϵ is diagonal in the Cartesian frame with $\epsilon_{xx} = \epsilon_{yy} = \epsilon_{zz}$. For *w*-BN and *h*-BN, the dielectric tensors are diagonal and have two independent components ϵ_{\parallel} and ϵ_{\perp} along and perpendicular to the *c* axis, respectively. Our results for the dielectric properties of the three BN modifications are presented in Table 3. For *c*-BN and *w*-BN, an overall excellent agreement between our calculations and experimental results is reached. In the case of *h*-BN, there are relatively large deviations concerning the perpendicular components. Our calculated values are 2.95 for the electric dielectric constant and 3.57 for the static dielectric constant, whereas the corresponding reported values in Ref. [3] were 4.1 and 5.06. However, our results are consistent with Refs. [7,26]. The differences in comparison with the former experimental values may be for two

Table 2

The optical phonon frequencies (in cm^{-1}) at the Γ point of the three polytypes of BN

Material	Mode	Present	Expt. ^a	Expt. ^b	Expt. ^c	Calc. ^d
<i>c</i> -BN	T_2	1027/1269	1056/1304			1062/1295
<i>w</i> -BN	A_1	1001/1249				1043/1280
	E_1	1041/1267				1075/1293
	E_2	476				475
	E_2	938				979
<i>h</i> -BN	A_{2u}	746/819		783/828		754/823
	E_{1u}	1372/1610		1367/1610		1382/1614
	E_{2g}	59			52	50
	E_{2g}	1372		1370	1366	1382

Two numbers in a row correspond to TO/LO frequencies.

^a Ref. [22].^b Ref. [3].^c Ref. [23].^d Ref. [7].

Table 3

Calculated dielectric properties for three polytypes of BN: macroscopic dielectric constant ϵ_∞ , static dielectric constant ϵ_0

Material	ϵ_\perp^∞	$\epsilon_\parallel^\infty$	ϵ_\perp^0	ϵ_\parallel^0	
<i>c</i> -BN	4.52	4.52	6.93	6.93	Present
	4.46	4.46	6.8	6.8	Expt. ^a
	4.54	4.54	6.74	6.74	Calc. ^b
<i>w</i> -BN	4.49	4.64	6.67	7.25	Present
	4.50	4.67			Calc. ^c
<i>h</i> -BN	4.87	2.95	6.71	3.57	Present
	4.95	4.1	6.85	5.06	Expt. ^d
	4.85	2.84	6.61	3.38	Calc. ^b

^a Ref. [24].^b Ref. [7].^c Ref. [25].^d Ref. [3].

reasons: (a) DFT in LDA or GGA is not appropriate to describe the weak interactions in *h*-BN, as mentioned above; and (b) Poor quality of *h*-BN samples were used in the IR reflectivity measurements in Ref. [3], as discussed below.

The dielectric constant of a material as a function of frequency ω is given by [27]

$$\epsilon(\omega) = \epsilon_\infty + \epsilon_\infty \sum_m \frac{\omega_{\text{LO},m}^2 - \omega_{\text{TO},m}^2}{\omega_{\text{TO},m}^2 - \omega^2 + i\gamma\omega} \quad (1)$$

where ϵ_∞ is the electronic contribution to ϵ , the sum is over IR-active phonon modes m , γ is the damping coefficient, $\omega_{\text{TO},m}$ and $\omega_{\text{LO},m}$ are their transverse optic (TO) and longitudinal optic (LO) mode frequencies, respectively. From the zero-frequency limit of Eq. (1), ϵ_0 can be separated into contributions arising from purely electronic screening ϵ_∞ and IR-active phonon modes according to

$$\epsilon_0 = \epsilon_\infty + \epsilon_\infty \sum_m \frac{\omega_{\text{LO},m}^2 - \omega_{\text{TO},m}^2}{\omega_{\text{TO},m}^2}. \quad (2)$$

The IR active mode frequencies and the corresponding contributions to the dielectric tensor are displayed in Table 4. It can be seen that for both polarized directions of the three polytypes, only one IR active mode makes contribution to

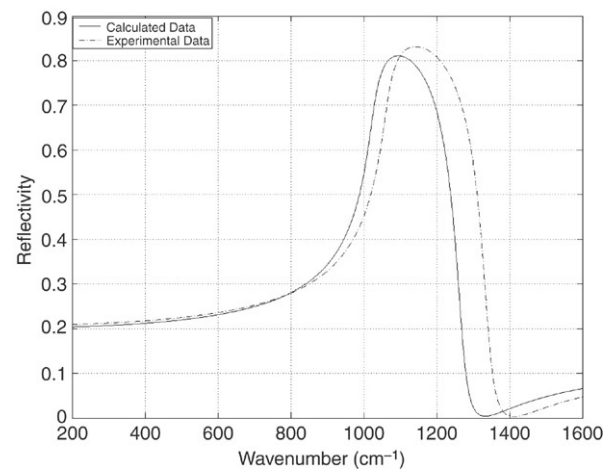


Fig. 1. Frequency dependence of the infrared reflectance for *c*-BN. The dash-dot line represents the experimental spectrum. The calculated data are given by the solid line. The damping was chosen to be 3% of the frequency for each mode.

the static dielectric constant. The zinc-blende and wurtzite structures, which differ only in the stacking order of double layers of the atoms, have almost the same lattice dielectric constant, with $\epsilon_\parallel^{\text{lat}} = \epsilon_\perp^{\text{lat}} = 2.38$ for *c*-BN and $\epsilon_\parallel^{\text{lat}} = 2.58$ and $\epsilon_\perp^{\text{lat}} = 2.16$ for *w*-BN. For all the modifications, contributions from the electronic polarizations are more than two times larger than those from the lattice vibrations.

The infrared reflectivity can be obtained from complex dielectric response $\epsilon(\omega)$ via

$$R(\omega) = \left| \frac{\sqrt{\epsilon(\omega)} - 1}{\sqrt{\epsilon(\omega)} + 1} \right|^2. \quad (3)$$

In Figs. 1 and 2 we present our predicted reflectivity $R(\omega)$ spectrum of *c*-BN and *h*-BN, compared with the experimental spectra measured in Refs. [4,3]. The damping constant has been chosen for each mode to be 3% of the frequency. It should be noted that two reststrahlen bands for the reflectivity and two active modes for each direction of polarization were found in Ref. [3] in their infrared investigations on *h*-BN. The group theoretical analysis shows that only one mode corresponding to one reststrahlen band for each direction (A_{2u} for $E \parallel c$ and

Table 4

LO/TO splittings and mode contributions to the component of dielectric tensor of *c*-BN, *w*-BN and *h*-BN

Phonon frequency (cm^{-1})							
Material	Mode	$E = 0$	$E \parallel a - b$	$E \parallel c$	$\sqrt{\Delta\omega^2}$ (cm^{-1})	$\epsilon_{\perp}^{\text{lat}}$	$\epsilon_{\parallel}^{\text{lat}}$
<i>c</i> -BN	T_2	1027	1269	1269	745.4	2.38	2.38
<i>w</i> -BN	A_1	1001	1001	1249	747	0	2.58
	E_1	1041	1267	1041	722	2.16	0
<i>h</i> -BN	A_{2u}	746	746	819	338	0	0.61
	E_{1u}	1372	1610	1372	842	1.83	0

The first column ($E = 0$) is for no electric field, the second is for the field lying in the plane ($E \parallel a - b$), and the third is for $E \parallel c$. The component of lattice dielectric constant parallel (perpendicular) to the *c*-axis is denoted $\epsilon_{\parallel}^{\text{lat}}$ ($\epsilon_{\perp}^{\text{lat}}$). $\Delta\omega^2 = \omega_{\text{LO}}^2 - \omega_{\text{TO}}^2$.

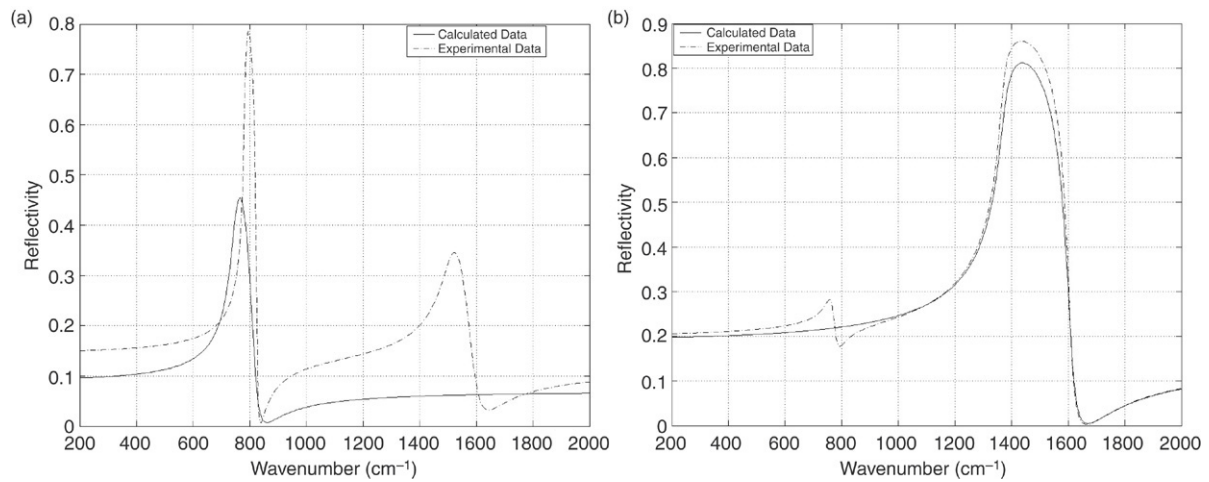


Fig. 2. Calculated (solid line) and experimental (dashdot line) reflectivity spectrum $R(\omega)$ for *h*-BN. The damping was chosen to be 3% of the frequency for each mode. (a) Polarization along the *c* axis. (b) Polarization in the *a-b* layer.

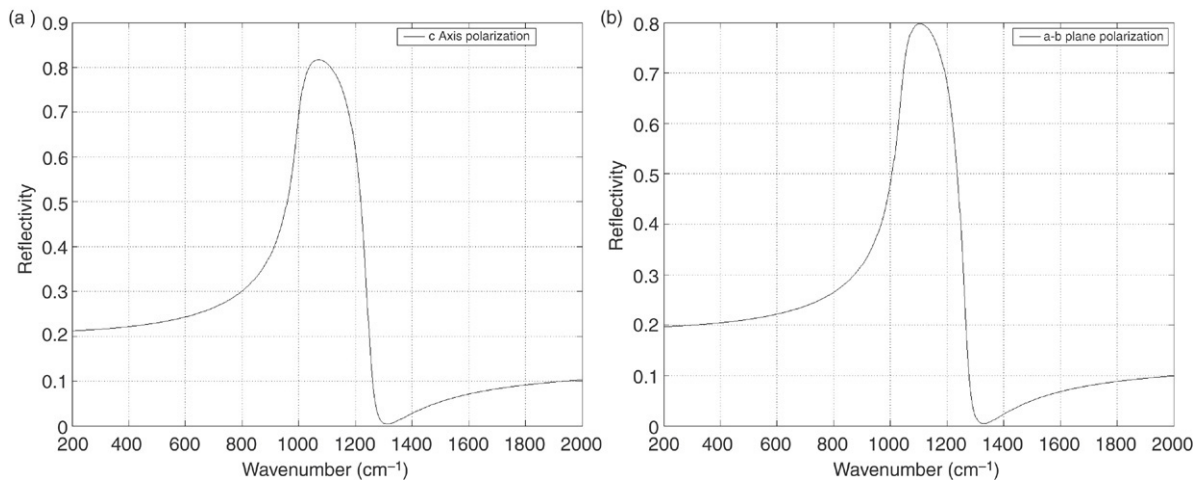


Fig. 3. Calculated reflectivity spectrum $R(\omega)$ for *w*-BN. The damping was chosen to be 3% of the frequency for each mode. (a) Polarization along the *c* axis. (b) Polarization in the *a-b* layer.

E_{1u} for $E \perp c$) should be expected. The weaker modes in the infrared spectra, according to the analysis of the authors, may probably be due to the misorientation in their polycrystalline sample, which may also lead to some uncertainty in the result of the dielectric constant measurement. In Fig. 3, we display our calculated reflectivity $R(\omega)$ spectrum for *w*-BN. Our theoretical

results suggest that *w*-BN should show a similar reflectivity spectrum as *c*-BN. It is difficult to distinguish the wurtzite structure from the zinc blende phase by IR spectroscopy. No IR spectrum has been reported for comparison; however, it is highly desirable to obtain polarized single-crystal IR data to confirm our predictions.

4. Conclusion

We have presented a first-principles study of the vibrational and dielectric properties for *c*-BN, *w*-BN and *h*-BN. Firstly, the structural parameters are optimized to obtain the minimal energy structural model, and an overall agreement has been reached between our theoretically calculated results and previous experiments ones, except for the lattice constant *c* of *h*-BN. The vibrational frequencies at the center of the Brillouin zone are evaluated. Then the dielectric tensors are obtained. The mode contributions to the static dielectric tensors are also presented. We find that all the structures have smaller lattice dielectric constants than their electronic contributions. Finally, the infrared reflectance spectrums are reported.

Acknowledgements

The authors acknowledge support from the Natural Science Foundation of China (Contract No. 90405015), from the National Young Elitists Foundation (Contract No. 50425208) and from the Program for Changjiang Scholars and Innovative Research Team in university (PCSIRT). We thank Northwestern Polytechnical University High performance Computing Center for allocation of computing time on their machines.

References

- [1] L. Liu, Y.P. Feng, Z.X. Shen, Phys. Rev. B 68 (2003) 104102.
- [2] V.L. Solozhenko, J. Hard Mater. 6 (1995) 51.

- [3] R. Geick, C.H. Perry, G. Ruppert, Phys. Rev. 146 (1966) 543.
- [4] P.J. Gielisse, S.S. Mitra, J.N. Plendl, R.D. Griffis, L.C. Mansur, R. Marshall, E.A. Pascoe, Phys. Rev. 155 (1967) 1039.
- [5] G. Cappellini, G. Satta, M. Palummo, G. Onida, Phys. Rev. B 64 (2001) 035104.
- [6] J.B. MacNaughton, et al., Phys. Rev. B 72 (2005) 195113.
- [7] N. Ohba, K. Miwa, N. Nagasako, A. Fukumoto, Phys. Rev. B 63 (2001) 115207.
- [8] M.D. Segall, P.J.D. Lindan, M.J. Probert, C.J. Pickard, P.J. Hasnip, S.J. Clark, M.C. Payne, J. Phys. Condens. Matter 14 (2002) 2717.
- [9] G.J. Ackland, M.C. Warren, S.J. Clark, J. Phys. Condens. Matter 9 (1997) 7861.
- [10] D.R. Hamann, M. Schlüter, C. Chiang, Phys. Rev. Lett. 43 (1979) 1494.
- [11] D.M. Ceperley, B.J. Alder, Phys. Rev. Lett. 45 (1980) 566.
- [12] S.H. Vosko, L. Wilk, M. Nusair, Canad. J. Phys. 58 (1980) 1200.
- [13] H.J. Monkhorst, J.D. Pack, Phys. Rev. B 13 (1976) 5188.
- [14] S. Baroni, S. de Gironcoli, A. Dal Corso, P. Giannozzi, Rev. Modern Phys. 73 (2001) 515.
- [15] X. Gonze, Phys. Rev. B 55 (1997) 10 337.
- [16] X. Gonze, C. Lee, Phys. Rev. B 55 (1997) 10 355.
- [17] R. Pick, M.H. Kohen, R.M. Martin, Phys. Rev. B 1 (1970) 910.
- [18] R.H. Wentorf Jr., J. Chem. Phys. 26 (1957) 956.
- [19] T. Soma, S. Sawaoka, S. Saito, Mater. Res. Bull. 9 (1974) 755.
- [20] V.L. Solozhenko, G. Will, F. Elf, Solid State Commun. 96 (1995) 1.
- [21] L. Wirtz, A. Rubio, Solid State Commun. 131 (2004) 141.
- [22] O. Brafman, G. Lengyel, S.S. Mitra, Solid State Commun. 6 (1968) 523.
- [23] T. Kuzuba, K. Era, T. Ishii, T. Sato, Solid State Commun. 25 (1978) 863.
- [24] M.I. Eremets, et al., Phys. Rev. B 52 (1995) 8854.
- [25] K. Karch, F. Bechstedt, Phys. Rev. B 56 (1997) 7404.
- [26] Y.-N. Xu, W.Y. Ching, Phys. Rev. B 44 (1991) 7787.
- [27] V. Železný, et al., Phys. Rev. B 66 (2002) 224303.